The Effects of Gas Nitriding on Fatigue Behavior in Titanium and Titanium Alloys

K. Tokaji, T. Ogawa, and H. Shibata

(Submitted 3 February 1998; in revised form 3 December 1998)

Fatigue behavior has been studied on gas-nitrided smooth specimens of commercial pure titanium, an alpha/beta Ti-6Al-4V alloy, and a beta Ti-15Mo-5Zr-3Al alloy under rotating bending, and the obtained results were compared with the fatigue behavior of annealed or untreated specimens. It was found that the role of the nitrided layer on fatigue behavior depended on the strength of the materials. Fatigue strength was increased by nitriding in pure titanium, while it was decreased in the Ti-6Al-4V and Ti-15Mo-5Zr-3Al alloys. Based on detailed observations of fatigue crack initiation, growth, and fracture surfaces, the improvement and the reduction in fatigue strength by nitriding in pure titanium and both alloys were primarily attributed to enhanced crack initiation resistance and to premature crack initiation of the nitrided layer, respectively.

Keywords crack growth, crack initiation, fatigue strength, gas nitriding, pure titanium, titanium alloy

1. Introduction

Pure titanium and titanium alloys have been widely used in the chemical and the aircraft industries because of their excellent corrosion resistance and high specific strength. In contrast to these advantages, however, they have a high coefficient of friction and poor wear resistance (Ref 1). These are the major problems in their application to critical machine components that come into contact with other metals and cause friction. To improve such tribological properties, a variety of surface engineering techniques such as gas nitriding (Ref 1-5), laser nitriding (Ref 1, 6), and ion implantation (Ref 7) have been successfully applied. Of these techniques, gas nitriding is considered to be the most promising method available for engineering applications because it can easily form a harder nitrided layer on the surface of the materials. By this method, substantial improvement in wear resistance can be achieved (Ref 1-3, 5). Conversely, such surface treatments have been reported to cause the decrease in the fatigue strength of titanium alloys (Ref 1, 5, 6). However, the reason for the reduction in fatigue strength and the fracture mechanisms have not been studied in detail.

In the present study, rotating bending fatigue tests were conducted using gas-nitrided smooth specimens of pure titanium, an alpha/beta Ti-6Al-4V alloy, and a beta Ti-15Mo-5Zr-3Al alloy. The obtained results were compared with the fatigue behavior of annealed or untreated specimens. The effects of gas nitriding on fatigue behavior are discussed on the basis of detailed observations of fatigue crack initiation, growth, and fracture surfaces.

K. Tokaji, Faculty of Engineering, Gifu University, 1-1 Yanagido, Gifu 501-1193, Japan; **T. Ogawa,** College of Science and Engineering, Aoyama Gakuin University, 6-16-1 Chitosedai, Setagaya-ku, Tokyo 157-8572, Japan; and **H. Shibata,** Gifu Prefectural Industrial Research Technical Centre, Kitaoyobi, Kasamatsu-cho, Hashima-gun, Gifu 501-6064, Japan. Contact e-mail: tokaji@mech.gifu-u.ac.jp.

2. Experimental Procedures

2.1 Materials and Nitriding Process

The materials used were commercial pure titanium, an alpha/beta Ti-6Al-4V alloy, and a beta Ti-15Mo-5Zr-3Al alloy. Their chemical compositions (weight percent) were 0.043 Fe, 0.095 O, 0.008 N, 0.0019 H, remainder Ti; 6.27 Al, 4.27 V, 0.206 Fe, 0.185 O, 0.003 N, 0.015 C, <0.001 Y, 0.0055 H, remainder Ti; and 3.01 Al, 14.51 Mo, 5.05 Zr, 0.042 Fe, 0.114 O, 0.0045 N, <0.001 H, remainder Ti, respectively. Smooth specimens with an 8 mm diameter and a 10 mm gage length were machined from the materials, mechanically polished by emery paper, and electropolished. Subsequently, they were nitrided and heat treated, as shown in Table 1.

In pure titanium, nitriding was performed at 850 and 1000 °C for 9 h, designated hereafter N850 and N1000, respectively. For a direct comparison with the nitrided specimens, untreated

Table 1 Heat treatment conditions

Alloy	Heat treatment	Specimen code	Depth of nitrided layer (d_n), μm
Pure titanium	Annealed at 700 °C for 1 h	A700	…
	Annealed at 850 °C for 9 h	A850	…
	Nitrided at 850 °C for 9 h	N850	20-30
	Annealed at 1000 °C for 9 h	A1000	…
	Nitrided at 1000 °C for 9 h	N1000	50-60
Ti-6Al-4V	Solution treated at 950 °C for 1 h and aged at 540 °C for 4 h	STA	…
	Annealed at 850 °C for 4 h	A4	…
	Nitrided at 850 °C for 4 h	N4	25
	Annealed at 850 °C for 15 h	A15	…
	Nitrided at 850 °C for 15 h	N15	65
Ti-15Mo-5Zr-3Al	Annealed at 750 °C for 20 h	A20	…
	Nitrided at 750 °C for 20 h	N20	130
	Annealed at 750 °C for 60 h	A60	…
	Nitrided at 750 °C for 60 h	N60	200

STA, solution treated and aged

specimens were prepared; they were annealed at the same temperature and period as the nitrided specimens (A850 and A1000). Specimens annealed at 700 °C for 1 h (A700) were also used to obtain a standard fatigue strength of the material.

For the Ti-6Al-4V and Ti-15Mo-5Zr-3Al alloys, 850 and 750 °C below the transformation temperatures were used as nitriding temperatures, respectively, because remarkable grain growth in the core material can be avoided. Prior to the fatigue test, the depth of the nitrided layers was examined by hardness measurements, and Fig. 1 shows the obtained results as a function of the nitriding period. It can be seen that the nitrided layer becomes deeper with increasing the nitriding period. Similar results have been reported for pure titanium (Ref 2) and a Ti-5Al-2.5Sn alloy (Ref 5).

Based on the results of Fig. 1, the nitriding periods of 4 and 15 h were chosen for Ti-6Al-4V alloys, which are designated N4 and N15. Specimens subjected to the same heat history as the nitrided specimens were also prepared for comparison (A4 and A15). In addition, specimens solution treated at 950 °C for 1 h followed by aging at 540 °C for 4 h were used to obtain a standard fatigue strength of the alloy.

For the Ti-15Mo-5Zr-3Al alloy, the nitriding periods of 20 and 60 h were employed (N20 and N60). Annealed specimens (A20 and A60) with the same heat history as the nitrided specimens were used.

Nitriding was performed in an electric furnace, which was evacuated before heating to nitriding temperatures; then nitrogen gas with a purity of 99.99% was admitted into it. Specimens were maintained for a given nitriding period under a constant nitrogen gas pressure of 0.13 MPa.

2.2 Mechanical Properties

Table 2 lists the mechanical properties. In pure titanium, the proof stress is higher, and the elongation and reduction of area are lower in the nitrided specimens than in the annealed specimens. In the Ti-6Al-4V alloy, monotonic strengths are slightly decreased by nitriding for 4 h, but are increased by nitriding for 15 h, while in the Ti-15Mo-5Zr-3Al alloy they are considerably reduced.

2.3 Procedures

Experiments were conducted on a 98 N·m rotating bending fatigue testing machine operating at a frequency of 57 Hz in laboratory air at room temperature. Crack initiation and growth were monitored by replicating the specimen surface. Fracture

Table 2 Mechanical properties

Alloy	Specimen code	0.2% proof stress ($\sigma_{0.2}$), MPa	Tensile strength (σ_B), MPa	Elongation (ϕ), %	Reduction of area (ψ), %
Pure titanium	A700	324	434	28	57
	A850	246	383	39	69
	N850	263	384	36	64
	A1000	317	409	34	58
	N1000	356	437	28	42
Ti-6Al-4V	STA	1132	1238	9	40
	A4	927	971	7	49
	N4	890	943	11	40
	A15	900	950	7	48
	N15	925	974	13	45
Ti-15Mo-5Zr-3Al	A20	957	1015	13	41
	N20	871	916	11	46
	A60	975	1001	13	40
	N60	875	901	12	47

STA, solution treated and aged

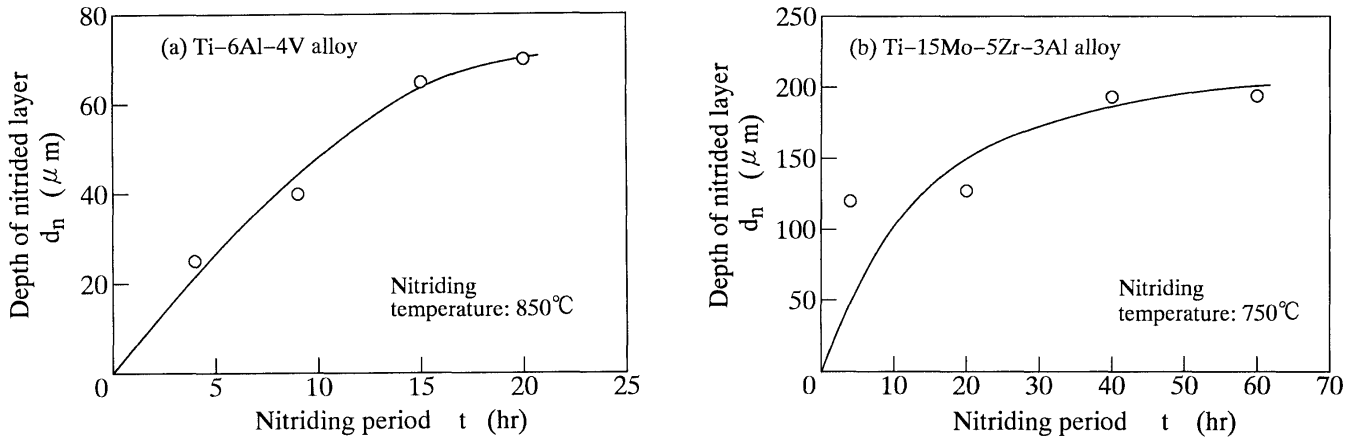

Fig. 1 Variations of depth of nitrided layer with nitriding period. (a) Ti-6Al-4V alloy. (b) Ti-15Mo-5Zr-3Al alloy

surfaces were examined using a scanning electron microscope (SEM).

3. Results

3.1 Nitrided Layer

Figure 2 shows the microstructures of the nitrided specimens in all the materials. The surface of the nitrided specimens had a golden color, and the intensity of the gold coloration tended to increase with increasing temperature or nitriding period. Thin compound TiN is seen on the specimen surface, and the nitrided layer of pure titanium can be identified clearly (Fig. 1a), while no discernible change in microstructure is seen in both alloys (Fig. 1b and c). Below the TiN layer, the layer of nitrogen-stabilized alpha solid solution is considered to be formed.

Figure 3 represents the normalized hardness on the cross section of the nitrided specimens, HV/HV_o, as a function of the distance from the specimen surface, where HV_o is the Vickers hardness of the core materials. In pure titanium (Fig. 3a), hardness increases within 20 to 30 μm and 50 to 60 μm from the surface for N850 and N1000, respectively. It also increases within 25 μm from the surface for N4 and 65 μm for N15 in the Ti-6Al-4V alloy (Fig. 3b), and 130 μm for N20 and 200 μm for N60 in the Ti-15Mo-5Zr-3Al alloy (Fig. 3c). These depths of the increased hardness can be considered as the nitrided layer. One

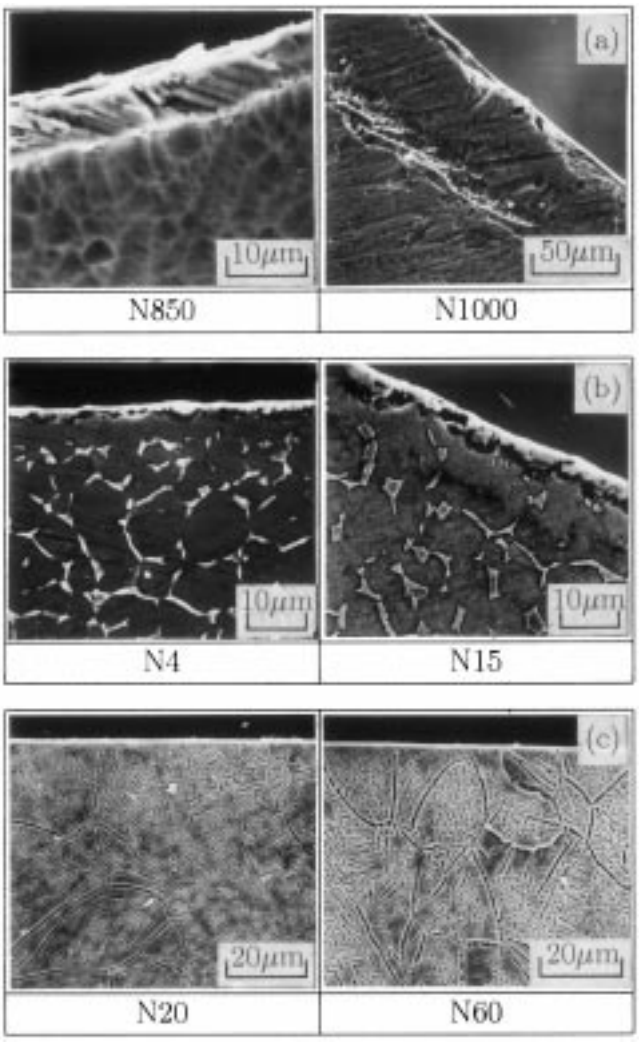

Fig. 2 Microstructures of nitrided materials. (a) Pure titanium. (b) Ti-6Al-4V alloy. (c) Ti-15Mo-5Zr-3Al alloy

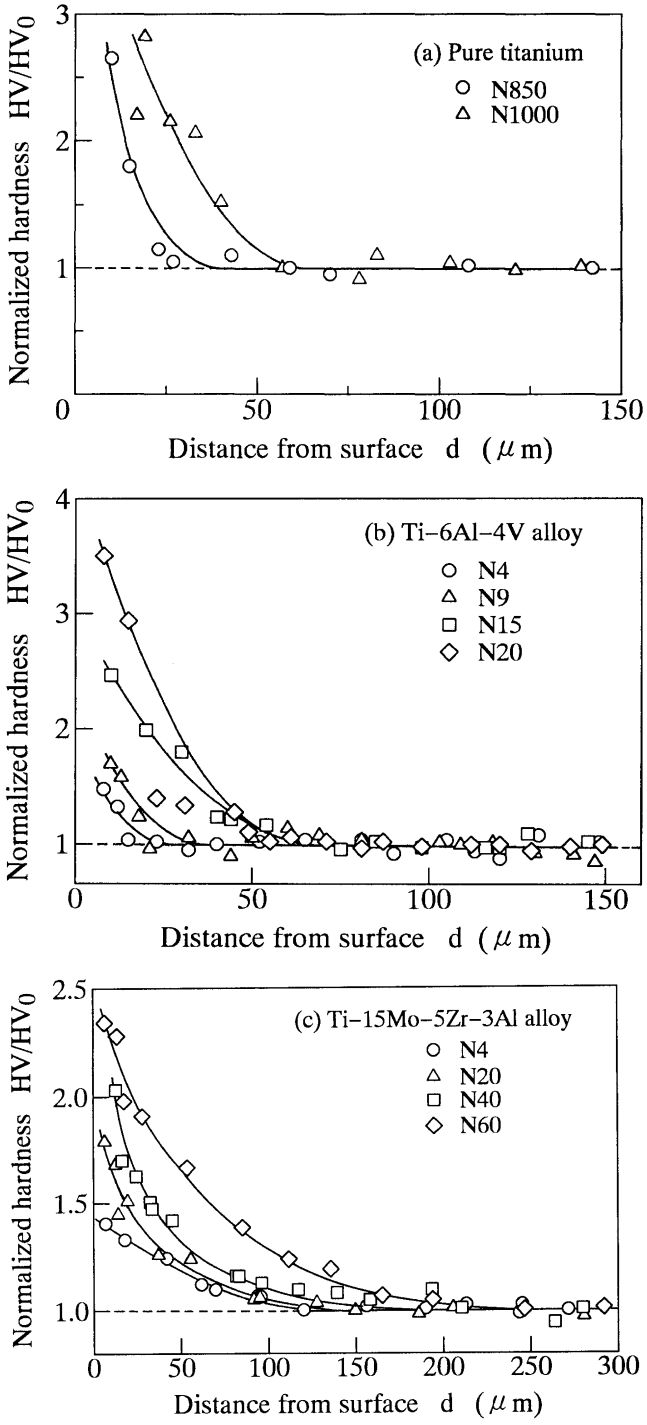

Fig. 3 Hardness profiles of nitrided materials. (a) Pure titanium. (b) Ti-6Al-4V alloy. (c) Ti-15Mo-5Zr-3Al alloy

further point to be noted from Fig. 3 is the increased hardness of the nitrided layer with an increase in temperature or nitriding period (Ref 2, 5). Because the HV_o values were 160 to 175 for pure titanium, 309 to 324 for the Ti-6Al-4V alloy, and 362 to 380 for the Ti-15Mo-5Zr-3Al alloy, the hardness on the specimen surface could be expected to be greater than 1000 HV.

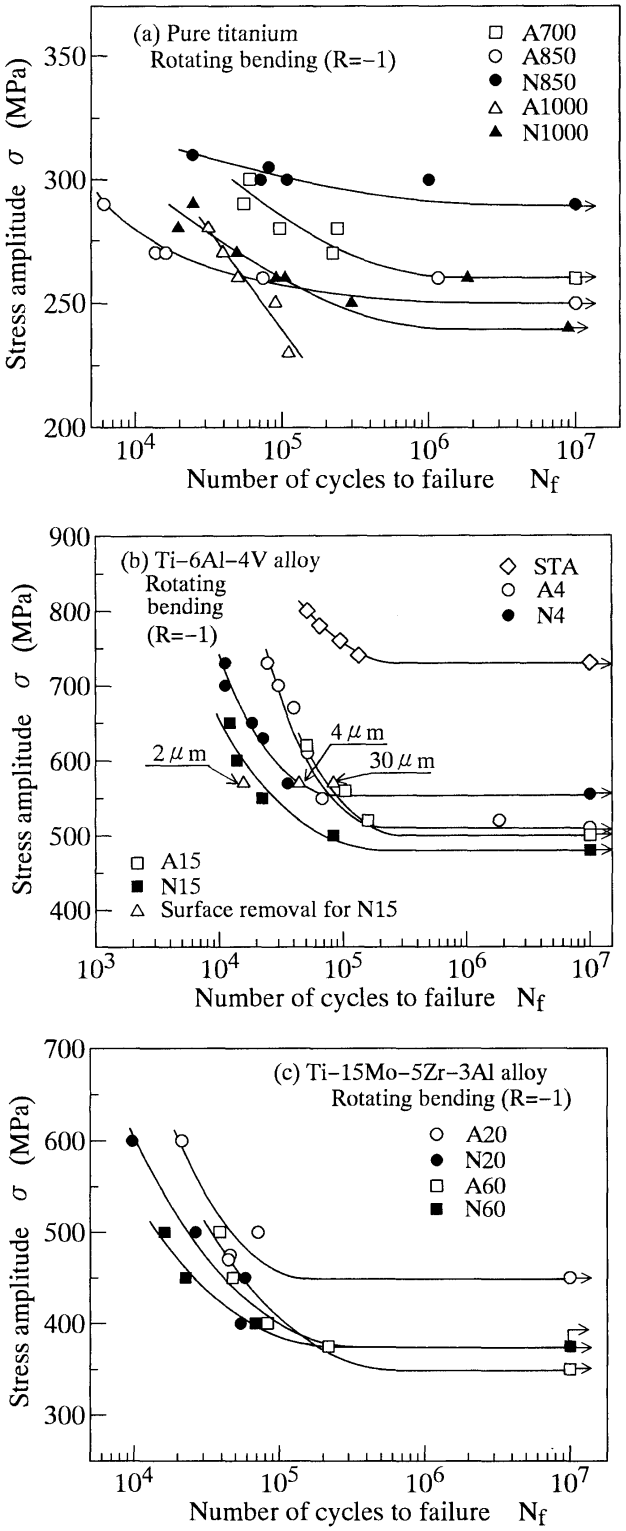

Fig. 4 Stress amplitude and number of cycles to failure (*S-N*) diagrams. (a) Pure titanium. (b) Ti-6Al-4V alloy. (c) Ti-15Mo-5Zr-3Al alloy

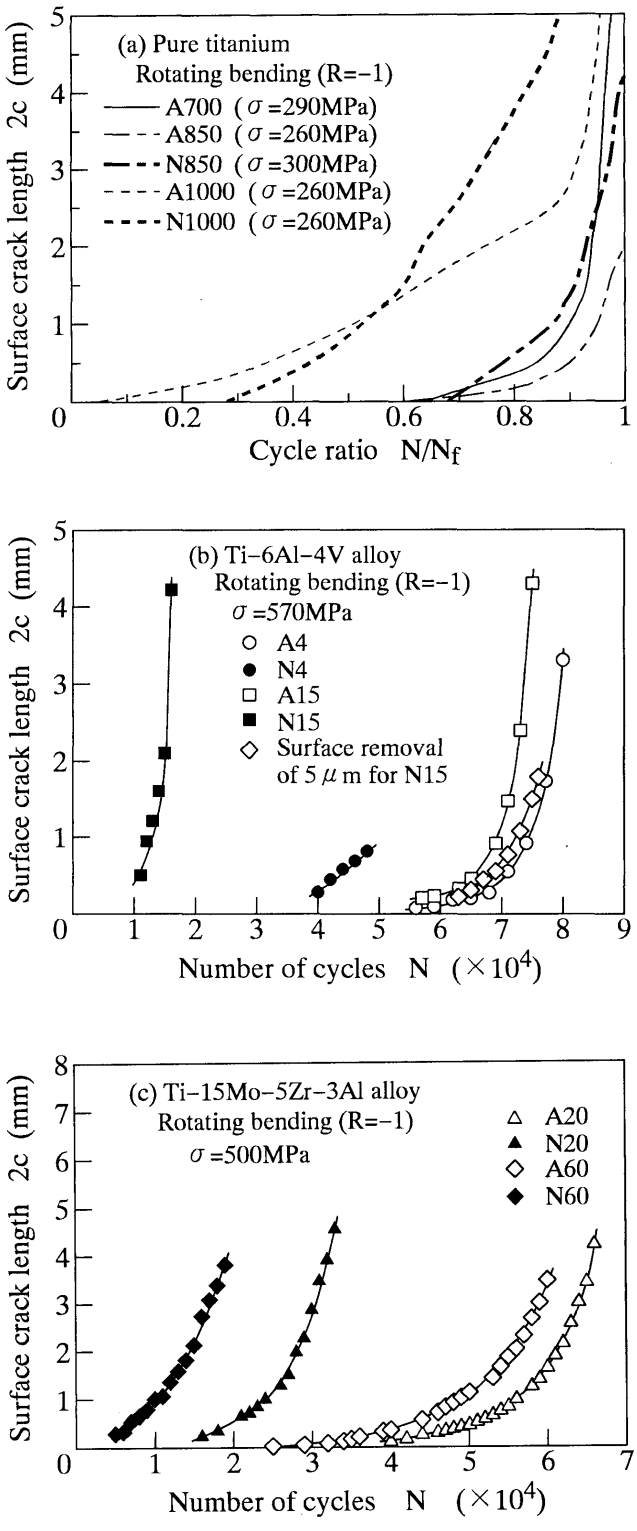

Fig. 5 Relationships between surface crack length and cycle ratio or number of cycles. (a) Pure titanium. (b) Ti-6Al-4V alloy. (c) Ti-15Mo-5Zr-3Al alloy

3.2 Fatigue Strength

Figure 4 shows the stress amplitude and number of cycles to failure (*S-N*) diagrams for all the materials. Figure 4(a) shows pure titanium. Figure 4(b) shows the Ti-6Al-4V alloy, and Fig. 4(c) shows the Ti-15Mo-5Zr-3Al alloy.

Pure Titanium. The fatigue strength of the annealed specimens tends to decrease with increasing annealing temperature, which is attributed to grain growth. It can be seen that the fatigue strength of the nitrided specimens, N850 and N1000, increases compared with that of the corresponding annealed specimens. In particular, the fatigue strength of N850 is remarkably improved and is superior to the standard strength of A700.

Ti-6Al-4V Alloy. The fatigue lives of N4 specimens are shorter than those of A4 specimens, but the fatigue limit is slightly increased. In contrast, the fatigue strength of N15 is reduced compared with A15 and is lower than that of N4, indicating that the harder and deeper nitrided layer has a detrimental effect on the fatigue strength (Ref 1, 5, 6).

Figure 4(b) also shows the fatigue results of N15 specimens, with surfaces that were removed by electropolishing. It is apparent that the fatigue lives gradually approach the life of A15 as the amount of removal increases. As the amount of removal corresponds to partial removal of the TiN layer (2 μm), complete removal of the TiN layer (4 μm), and removal of half the nitrided layer (30 μm), respectively, the TiN layer and the harder solid solution layer just below the surface are considered to be strongly related to the decrease in fatigue strength of the nitrided specimens.

Ti-15Mo-5Zr-3Al Alloy. Results similar to those for the Ti-6Al-4V alloy are obtained in this alloy. The fatigue strength of N20 decreases compared with A20, while the fatigue lives of N60 are shorter than those of A60. However, the fatigue limit is slightly increased.

It has been reported that fatigue strength is reduced by nitriding in Ti-6Al-4V alloys (Ref 1, 5, 6), and the present results also show the decrease in fatigue strength by nitriding in titanium alloys.

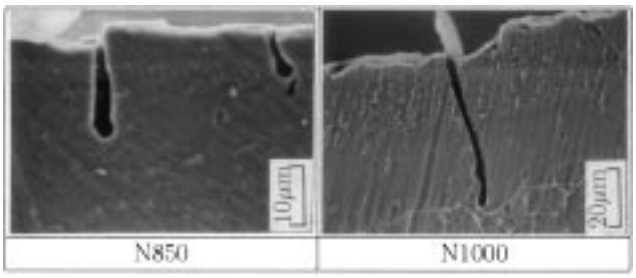

Fig. 6 Crack initiation and early growth into the bulk of nitrided specimens in pure titanium

3.3 Initiation and Growth of Fatigue Cracks

Figure 5 presents the relationships between surface crack length, 2*c*, and cycle ratio, N/N_f, or number of cycles, *N*.

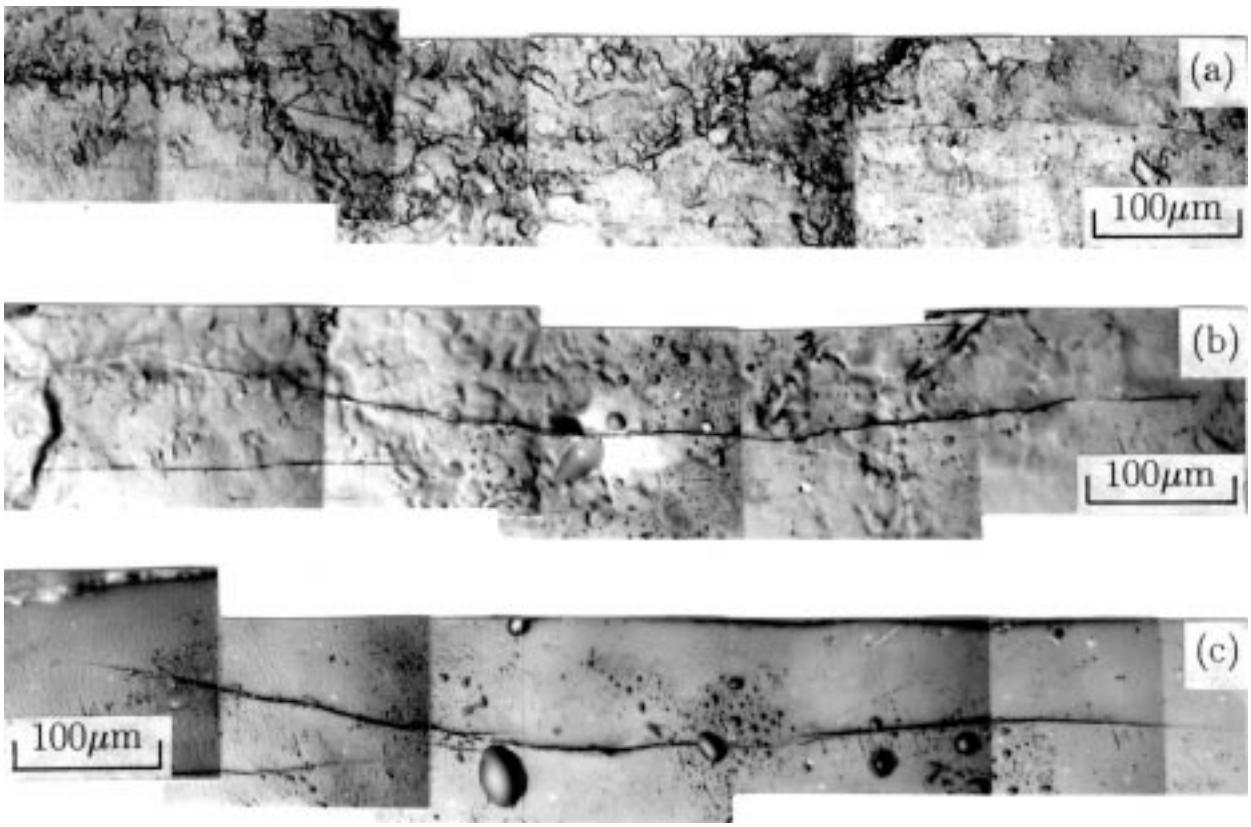

Fig. 7 Changes in crack morphology with removal of surface layer in N1000. (a) Surface. (b) 25 μm below the specimen surface (in nitrided layer). (c) 75 μm below the specimen surface (in core material)

Pure Titanium. Pure titanium showed the enhanced crack initiation resistance in the nitrided specimens compared with the annealed specimens (Fig. 5a). In the N850 specimen, crack initiation is relatively delayed by nitriding in spite of a higher cyclic stress applied, and no crack is initiated at σ = 260 MPa, which was applied for A850. Similarly, it can be seen from the figure that crack initiation in N1000 is also delayed.

Surface observation of crack growth indicated that cracks in the annealed specimens exhibited an extremely tortuous path due to the effect of microstructure, while cracks in the nitrided specimens revealed a straight morphology without any deflections. Figure 6 shows crack initiation and early crack growth in the bulk of the nitrided specimens, clearly revealing that cracks are initiated at the specimen surface, not at the boundary between the nitrided layer and the core material. As an example, Fig. 7 shows the change in crack morphology of a N1000 specimen with a surface that was gradually removed by electropolishing: (a), (b), and (c) are on the specimen surface, in the nitrided layer (25 μm removal) and in the core material (75 μm removal), respectively. The crack morphology is the same as on the specimen surface not only in the nitrided layer, but also in the core material. Similar appearance was observed for N850 specimens. From the observations of Figs. 6 and 7, cracks were initiated on the specimen surface in the nitrided specimens and then grew continuously into the core material.

Figure 8 presents the relationship between crack growth rate, *da*/*dN*, and maximum stress intensity factor, K_{max}. The N850 specimen shows lower *da*/*dN* than the A850 specimen over the entire K_{max} regime tested. In contrast, there is no noticeable difference in *da*/*dN* between the N1000 and A1000 specimens.

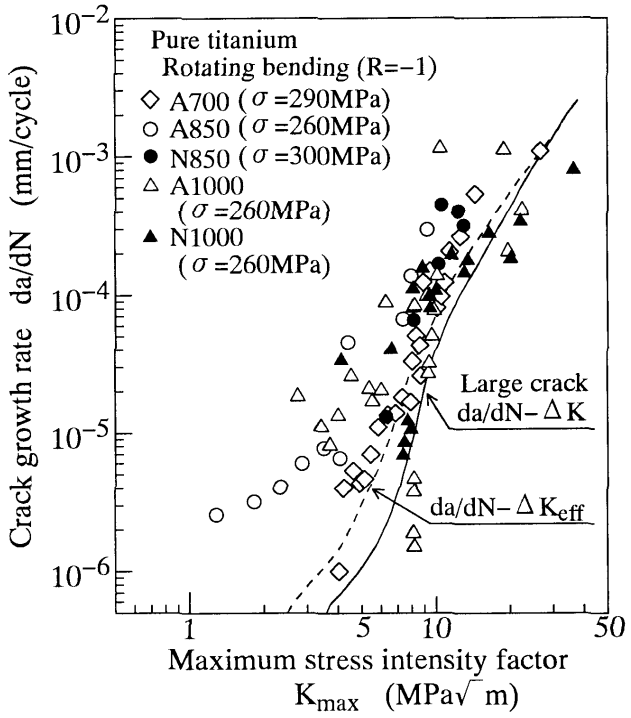

Fig. 8 Relationship between crack growth rate and maximum stress intensity in pure titanium

Figures 9 and 10 show scanning electron micrographs of fracture surfaces of N850 and N1000, respectively. In the N850 specimen (Fig. 9), the crack shape is nearly semicircular (Fig. 9a), but the traces of the crack tip indicated by the arrow in the magnified micrograph (Fig. 9b) suggest that at the early stage of crack growth the crack grows faster at the boundary between the nitrided layer and the core material than at the specimen surface. This observation gives evidence that the existence of the nitrided layer can enhance crack growth resistance. In the N1000 specimen (Fig. 10), however, such a feature is not observed, and the brittle nature of the nitrided layer can be seen (Fig. 10b). It is considered, therefore, that the effect of the nitrided layer on crack growth may be different depending on its property and depth.

Ti-6Al-4V Alloy. As can be seen in Fig. 5(b), the initiation resistance was lowered by nitriding; in particular, the N15 specimen showed a considerable decrease in crack initiation resistance. It should be noted that the specimen with a surface that was removed by 5 μm indicated the same initiation resistance as the corresponding annealed specimen. This result suggests that the TiN layer and the harder nitrided layer just below the surface are strongly related to premature crack initiation in the nitrided specimens.

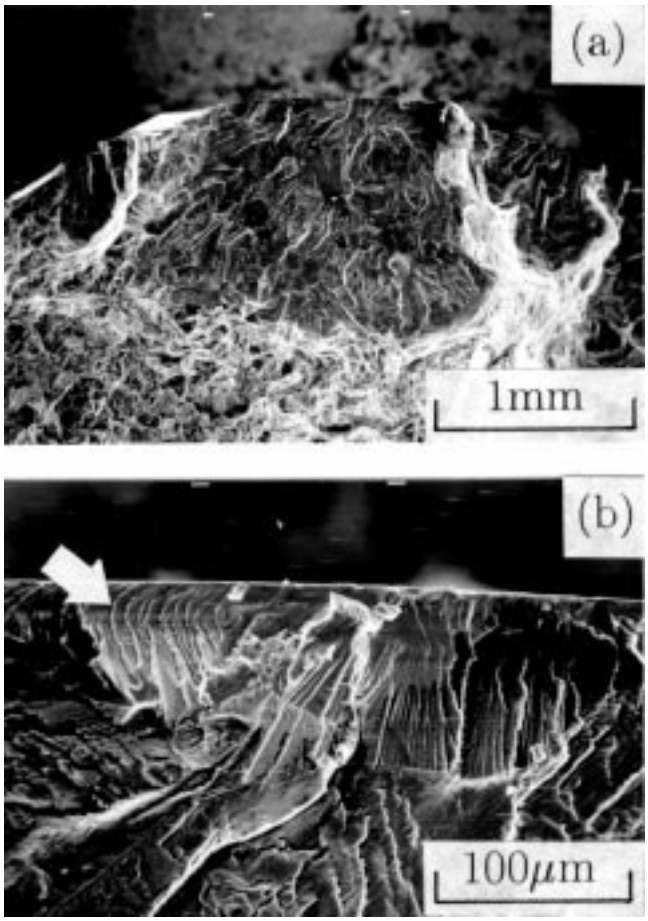

Fig. 9 Scanning electron micrographs of fracture surface in N850. (a) Macroscopic appearance. (b) Magnified view of crack initiation site

Unusual crack initiation behavior was observed in the nitrided specimens. In the N15 specimen, there were not cracks at $N = 1.0 \times 10^4$ cycles, but a crack of $2c = 498$ μm was initiated after only 10^3 cycles. To confirm the reproducibility of the behavior, the same observation was made on a different specimen. A crack of $2c = 1390$ μm was initiated at $N = 9 \times 10^3$ cycles. However, no crack was observed at $N = 8 \times 10^3$ cycles. The crack had already grown to the core material, but its depth, a, was only 133 μm, as shown in Fig. 11. Thus the aspect ratio, a/c, was extremely small. These observations suggest that a crack is initiated suddenly at a relatively large size or grows rapidly in the surface layer. As the crack grew into the core material and led to the final failure, premature crack initiation was primarily responsible for the reduction in fatigue strength for the nitrided specimens.

Figure 12 shows the aspect ratio as a function of $2c$. The a/c values decrease slightly with increasing $2c$ in the annealed specimens, while they are extremely small in the N15 specimen immediately after crack initiation, increase rapidly with increasing $2c$, and coincides with those of the annealed specimens in the region of the crack length of $2c \geq 3.2$ mm.

The relationships between surface crack growth rate, dc/dN, and $(K_{max})_C$ and crack growth rate into the bulk, da/dN, and $(K_{max})_A$ are presented in Fig. 13. As shown, da/dN is almost the same for the nitrided and annealed specimens (Fig. 13b), but dc/dN for the nitrided specimens is significantly faster than that for the annealed specimens (Fig. 13a), indicating that the hard nitrided layer can accelerate crack growth, which is more noticeable at smaller crack size.

Ti-15Mo-5Zr-3Al Alloy. The crack initiation resistance of N60 and N20 was decreased compared with A60 and A20. N60, having a harder and deeper nitrided layer, exhibits earlier crack initiation than N20 (see Fig. 5c). In the nitrided specimens, similar crack initiation behavior to the Ti-6Al-4V alloy was observed; thus the reduction in fatigue strength of the nitrided specimens can also be attributed to premature crack initiation at a relatively large size.

As a typical example, Fig. 14 shows scanning electron micrographs of fracture surfaces of the Ti-15Mo-5Zr-3Al alloy. There is a clear difference between the annealed and nitrided specimens. In the annealed specimen, radial markings originating from the crack initiation site are observed, and thus the

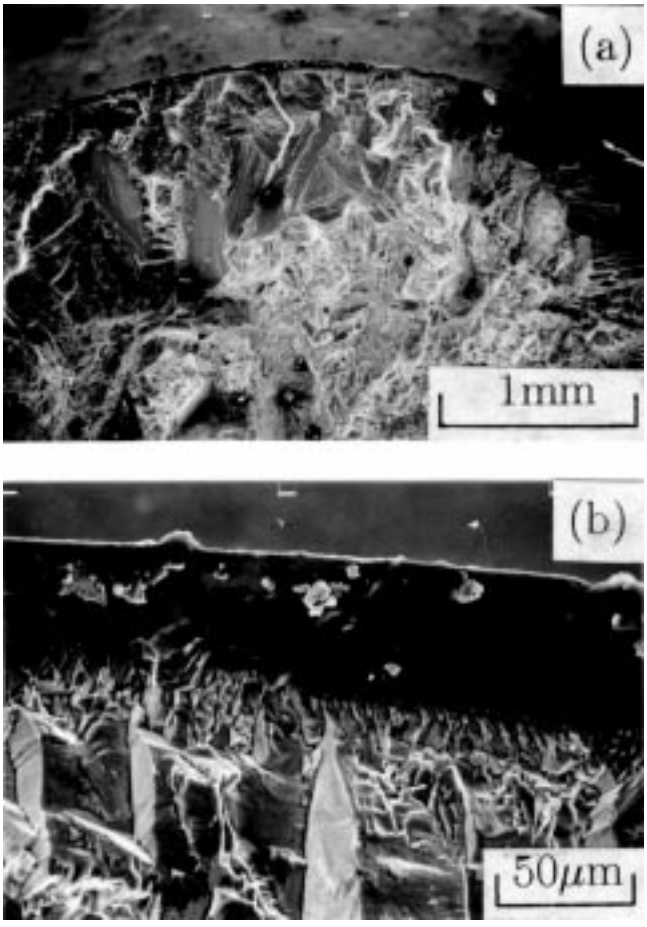

Fig. 10 Scanning electron micrographs of fracture surface in N1000. (a) Macroscopic appearance. (b) Magnified view of crack initiation site

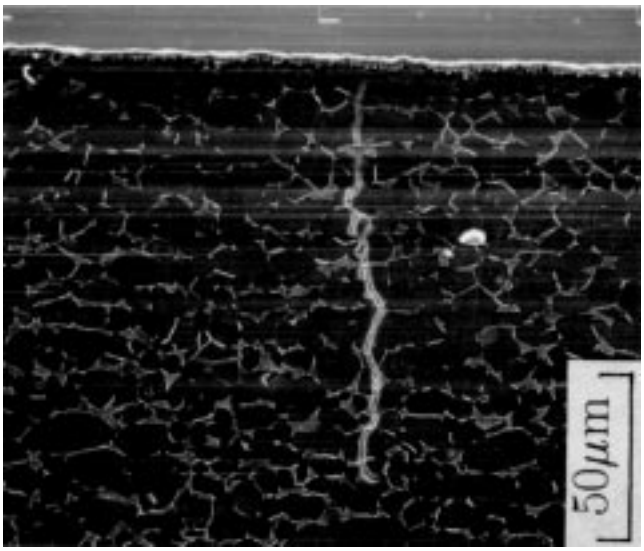

Fig. 11 Crack morphology inside of the specimen immediately after crack initiation in N15 ($2c = 1390$ μm, $a = 133$ μm)

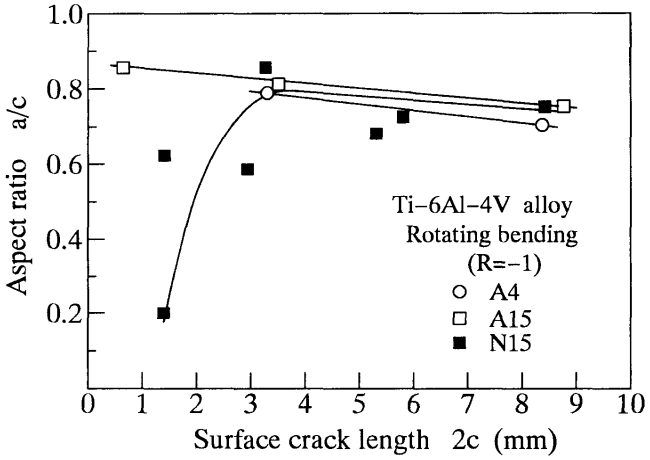

Fig. 12 Variation of aspect ratio with crack growth in Ti-6Al-4V alloy

crack is considered to grow concentrically. In the nitrided specimen, markings perpendicular to the specimen surface are observed, indicating that the crack is initiated suddenly at a relatively large size and grow into the bulk. These features were also observed in the Ti-6Al-4V alloy.

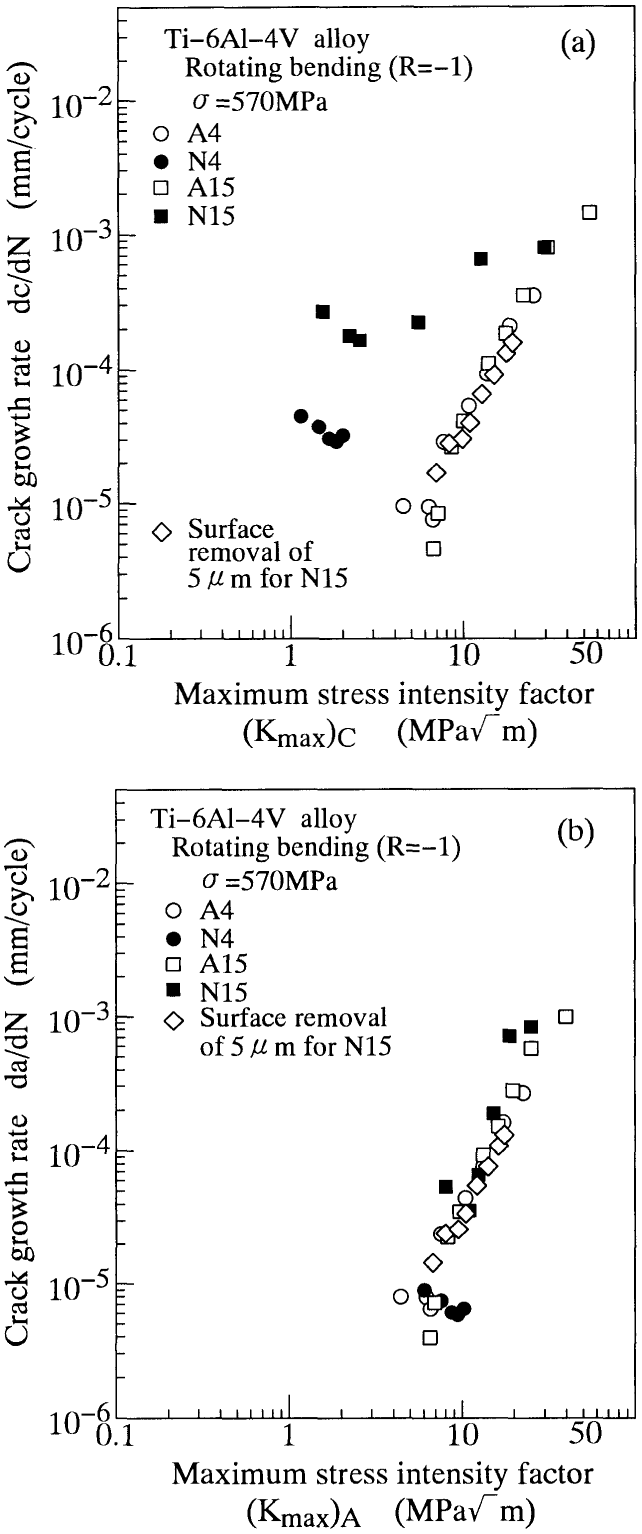

Fig. 13 Relationships between crack growth rate and maximum stress intensity in Ti-6Al-4V alloy. (a) Specimen surface. (b) Deepest point

4. Discussion

The fatigue strength of pure titanium was found to improve by nitriding. Because the material has to be kept at high temperatures for a long time during the nitriding process, grain growth takes place in the core material, and its fatigue strength is consequently decreased. However, a hard nitrided layer formed on the specimen surface can enhance the crack initiation resistance because of the constraint of cyclic plastic deformation of the core material. It has also been reported that TiN coating formed by chemical vapor deposition (CVD) and physical vapor deposition (PVD) enhanced the fatigue crack initiation resistance (Ref 8). Nitriding at 850 °C can also increase the crack growth resistance, as shown in Fig. 8. As a result, the fatigue strength of the nitrided specimens was improved compared with that of the corresponding annealed specimens.

In titanium alloys, although the fatigue limits were slightly improved by nitriding, the overall fatigue strength was reduced compared with the corresponding annealed specimens. It has

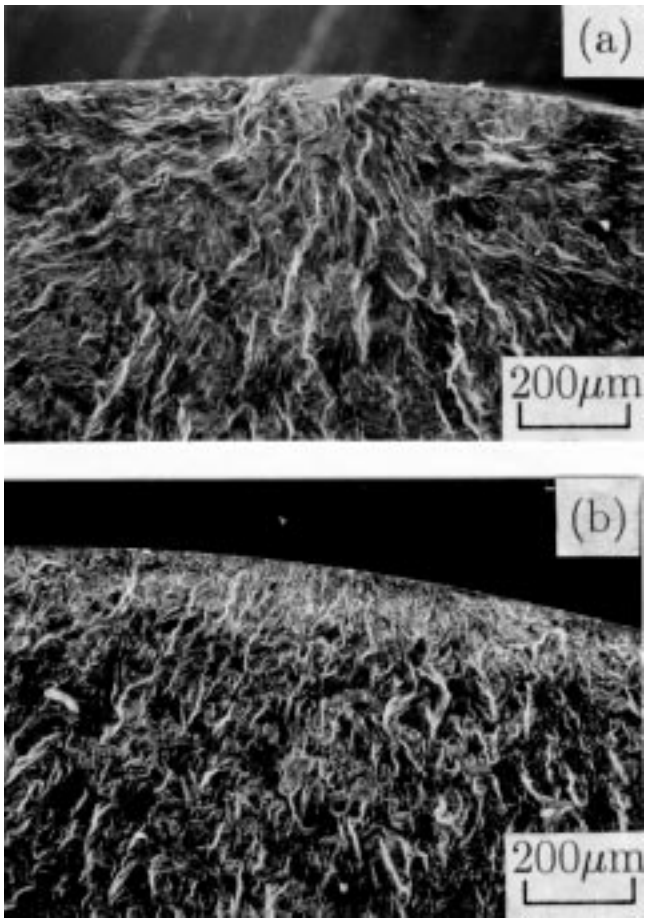

Fig. 14 Scanning electron micrographs of fracture surface in Ti-15Mo-5Zr-3Al alloy. (a) A60. (b) N60

been reported that the fatigue strength of Ti-6Al-4V alloys was decreased by nitriding (Ref 1, 5, 6). However, the reason for the reduction in fatigue strength has not been clarified because the emphasis was placed on the improvement of wear resistance. Furthermore, the conditions under which the fatigue strength of the reference comparison was obtained were unclear. During the nitriding process, the microstructure of the core materials can change. In general, the strength of titanium alloys is very sensitive to microstructure, and thus when the effect of the nitrided layer is discussed, comparison should be made with material subjected to the same heat history as the nitrided materials. In the present study, as the results for the nitrided specimens are compared with those of the corresponding annealed specimens with identical microstructure and grain size, the effect of nitriding can be evaluated exactly. If the fatigue strength of the nitrided specimens is compared with that of solution treated and aged (STA) specimens, which is one of the recommended heat treatments for Ti-6Al-4V alloys, then the nitrided specimens show a large reduction (see Fig. 4b).

It is evident from the results for the specimen with the surface that was gradually removed by electropolishing that the TiN layer and harder solid-solution layer below the specimen surface were strongly related to the reduction in fatigue strength because the crack initiation behavior of the specimen was almost the same as that of the annealed specimens. In addition, the crack shape of the nitrided specimens just after crack initiation was extremely shallow. This also indicates that the nitrided layer was related to premature and unusual crack initiation behavior observed in the titanium alloys, which was responsible for the reduction in fatigue strength of the nitrided specimens, in addition to the enhanced crack growth at the early stage.

As described previously, the nitrided layer plays the contrary roles in crack initiation behavior depending on material. This can be attributed to the difference in deformation between the nitrided layer and the core material. Because titanium alloys have high strengths and low elastic modulus, very large elastic deformation occurs during fatigue testing. The elastic modulus of the TiN layer is two to six times that of the core materials; thus the TiN layer is under severe deformation and subjected to high stress. When localized fatigue deformation takes place at the surface of the core material, brittle cracking results in the TiN layer and harder solid-solution layer. This is the unusual crack initiation behavior observed in the titanium alloys. Therefore, the shape of a crack, once initiated, becomes very shallow, and subsequent growth into the bulk occurs rapidly. Conversely, the strength of pure titanium was considerably lower than that of the alloys (see Table 2); thus elastic deformation during the fatigue test is small. In this case, the nitrided layer can prevent the initiation of slip and consequently enhance the resistance to fatigue crack initiation (Ref 8). Therefore, it is concluded that the role of the nitrided layer in crack initiation behavior can depend on the strength of materials.

5. Conclusions

Rotating bending fatigue tests were conducted using gas-nitrided smooth specimens of commercial pure titanium, a Ti-6Al-4V alloy, and a Ti-15Mo-5Zr-3Al alloy. The effects of gas nitriding on fatigue behavior and the fracture mechanisms were discussed. The following conclusions can be made:

- The depth and hardness of the nitrided layer increased with increasing nitriding temperature and period.
- In pure titanium, fatigue strength was increased by nitriding, while in the Ti-6Al-4V and Ti-15Mo-5Zr-3Al alloys, the overall fatigue strength tended to be reduced by nitriding.
- In pure titanium, the crack initiation resistance of the nitrided specimens was largely enhanced compared with the annealed specimens. In the Ti-6Al-4V and Ti-15Mo-5Zr-3Al alloys, premature crack initiation occurred at a relatively large size in the nitrided specimens; that is, the initiation resistance was significantly decreased by nitriding.
- There was a case where the crack growth resistance was enhanced by nitriding in pure titanium. The crack growth rates at the specimen surface in the nitrided specimens of the Ti-6Al-4V alloy were faster than those in the annealed specimens, especially at smaller crack size.
- The role of the nitrided layer on fatigue behavior depended on the strength of the materials. The improvement in fatigue strength by nitriding was attributed to the enhanced crack initiation resistance if the strength was low, as in pure titanium, while the reduction in fatigue strength was primarily due to premature crack initiation if the strength was high, as in the Ti-6Al-4V and Ti-15Mo-5Zr-3Al alloys.

Acknowledgments

The authors wish to thank H. Sekiya, Y. Matsunaga, and C. Asahara for nitriding treatment performed at the Gifu Prefectural Metal Research Institute. Thanks are also given to Y. Kamiya, G. Hisamatsu, and C. Hori for assistance with the experiments.

References

1. T. Bell, H.W. Bergmann, J. Lanagan, P.H. Morton, and A.M. Staines, Surface Engineering of Titanium with Nitrogen, *Surf. Eng.*,Vol 2 (No. 2), 1986, p 133-143
2. S. Yoshida and J. Isono, On the Nitriding of Titanium, *Kikaishikensho-shoho*, Vol 10 (No. 2), 1956, p 78-83 (in Japanese)
3. K. Nakano, S. Yamamato, H. Kobayashi, and A. Takamura, The Properties of Nitrided Titanium, *Trans. Jpn. Inst. Met.*, Vol 24 (No. 8), 1960, p 500-504 (in Japanese)
4. A. Takamura, Nitriding of Titanium, *Trans. Jpn. Inst. Met.*, Vol 24 (No. 9), 1960, p 565-569 (in Japanese)
5. E. Mitchell and P.J. Brotherton, Surface Treatments for Improving the Wear-Resistance and Friction Properties of Titanium and Its Alloys, *J. Inst. Met.*, Vol 93, 1965, p 381-386
6. B.L. Mordike and H.W. Bergmann, Surface Treatment of Titanium Using Lasers, *Mat. Res. Soc. Symp. Proc.*, Vol 58, 1986, p 335-341
7. R.G. Vardiman and R.A. Kant, The Improvement of Fatigue Life in Ti-6Al-4V by Ion Implantation, *J. Appl. Phys.*, Vol 53 (No. 1), 1982, p 690-694
8. K. Shiozawa and S. Ohshima, Effect of TiN Coating on Fatigue Strength of Carbon Steel, *J. Soc. Mater. Sci., Jpn.*, Vol 39 (No. 442), 1990, p 927-932 (in Japanese)